Microchimica Acta
https://doi.org/10.1007/s00604-018-3031-z

ORIGINAL PAPER

Colorimetric adenosine aptasensor based on DNA cycling amplification and salt-induced aggregation of gold nanoparticles

Caiyun Kong[1] · Linna Gao[2] · Zhengbo Chen[1]

Received: 7 September 2018 / Accepted: 27 September 2018

Abstract

An aptamer based assay is described for the colorimetric detection of adenosine. The presence of adenosine triggers the deformation of hairpin DNA oligonucleotide (HP1) containing adenosine aptamer and then hybridizes another unlabeled hairpin DNA oligonucleotide (HP2). This leads to the formation of a double strand with a blunt 3′ terminal. After exonuclease III (Exo III)-assisted degradation, the guanine-rich strand (GRS) is released from HP2. Hence, the adenosine-HP1 complex is released to the solution where it can hybridize another HP2 and initiate many cycles of the digestion reaction with the assistance of Exo III. This leads to the generation of a large number of GRS strands after multiple cycles. The GRS stabilize the red AuNPs against aggregation in the presence of potassium ions. If, however, GRS forms a G-quadruplex, it loses its ability to protect gold nanoparticles (AuNPs) from salt-induced AuNP aggregation. Therefore, the color of the solution changes from red to blue which can be visually observed. This colorimetric assay has a 0.13 nM detection limit and a wide linear range that extends from 5 nM to 1 μM.

Keywords Adenosine detecion · Hairpin DNA oligonucleotide · Low detection limit · Wide linear range · Colorimetric assay · Gold nanoparticle aggregation · Exonuclease III · Color change · G-quadruplex · DNA cycling amplification

Introduction

Adenosine is involved in neuromodulation [1], cell signaling [2], and neuroprotection [2]. In the brain, adenosine regulates cerebral blood flow and neurotransmission [3], offering an effective treatment means of ischaemia, epilepsy, inflammation, as well as chronic and neuropathic pain [4–6]. Therefore, it is very vital to detect adenosine for clinical diagnosis.

Massive detection methods have been developed for the determination of adenosine, such as fluorescence [7–9], electrochemiluminescence [10, 11], capillary electrophoresis [12], chromatography [13, 14], and surface-enhanced Raman spectroscopy [15]. However, some of the approaches have some disadvantages, such as expensive instruments, tedious sensing process, limited detection range, as well as weak selectivity ability.

To address these defects, aptamer biosensors have been developed for the highly sensitive and selective detection of adenosine [16–23]. Hereinto, gold nanoparticles (AuNPs) based colorimetric aptasensors stand out from these adenosine aptasensors due to advantages of its rapidness, simplicity, and no need to use expensive analytical instruments [24–30]. These aptasensor exhibited excellent specificity for adenosine, however, sensitivity still needs to be improved.

Here, we designed a sensitive colorimetric aptasensor based on AuNP aggregation for detecting adenosine (Scheme 1). This sensor involves two hairpin DNA oligonucleotides (HP1 and HP2), where HP1contains adenosine aptamer, and HP2 consists of the guanine-rich strand (GRS). With adenosine, the specific binding of HP1 to adenosine causes the deformation of hairpin-structured HP1, and further triggers HP1 and HP2 to hybridize to each other, thus forming a duplex DNA structure with a blunt 3′ end. Therefore, Exo III can recognize the blunt 3′ terminus and digest the segment (light blue) of HP2 [31, 32]. The adenosine-HP1 complex is released intact to hybridize with another HP2. After a series of

Electronic supplementary material The online version of this article (https://doi.org/10.1007/s00604-018-3031-z) contains supplementary material, which is available to authorized users.

✉ Zhengbo Chen
czb979216@sina.com

[1] Department of Chemistry, Capital Normal University, Beijing 100048, China

[2] College of Chemical and Environmental Engineering, Shandong University of Science and Technology, Qingdao 266590, China

Published online: 02 October 2018

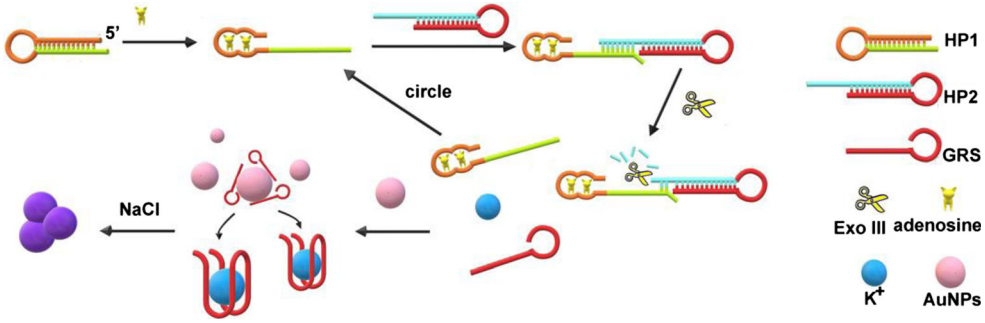

Scheme 1 Schematic illustration of the colorimetric aptasensor for adenosine detection based on Exo III-assisted DNA cycling amplification and G-quadruplex-induced AuNP aggregation in salt solution

Exo III-assisted cycles of DNA cleavage reaction, more amounts of GRS are generated. The binding of GRS to potassium ions prompts GRS to fold into stable G-quadruplex structure, thus preventing the stabilization of individual AuNPs, resulting in purple-blue AuNP aggregates under high salt conditions. Therefore, the target adenosine can be identified by the bare eye or quantified sensitively by UV-vis spectrometry. The above significant changes were confirmed by TEM images of the AuNPs at different conditions as shown in Fig. 1. As presented, the AuNPs are well-dispersed in aqueous solutions, whereas the presence of target adenosine caused AuNP aggregates.

Experimental section

Materials and reagents

Trisodium citrate, chloroauric acid ($HAuCl_4 \cdot 3H_2O$), Adenosine (A), uridine (U), cytidine (C), and Exonuclease III (Exo III) were purchased from Aladdin Industrial Corporation (www.aladdin.com, Shanghai, China). The DNA sequences (HP1: 5′- AGA GAA CCT GGG GGA GTA TTG CGG AGG AAG GTC GCA ATA CTC CCC CAG GTA TTT TTT-3′, HP2: 5'-TGC GAT GGG TTG GGC GGG ATG GGA ACC GCC CAA CCC ATC GCA ATA CCT GG-3′) were synthesized by Sangon Biotech Co., Ltd. (www.sangon.com, Shanghai, China). All of the reagents were of analytical reagent grade. Ultrapure water was provided by a Direct-Q3 system and used as a solvent in all experiments.

Instrumentation

UV-vis absorption spectra were recorded by a Shimadzu UV-2550 spectrophotometer (Japan). Transmission electron microscope (TEM) was performed on a JEM-2010 transmission electron microscope at 80 kV.

Synthesis of gold nanoparticles

The information is available in Supporting Information (Synthesis of gold nanoparticles, **Fig. S1**).

Protocol for adenosine detection

Prior to use, DNA strands were processed as follows: Hairpin HP1 (1 μM) and HP2 (1 μM) were respectively heated to 85 °C for 10 min, and then slowly cooled down to room

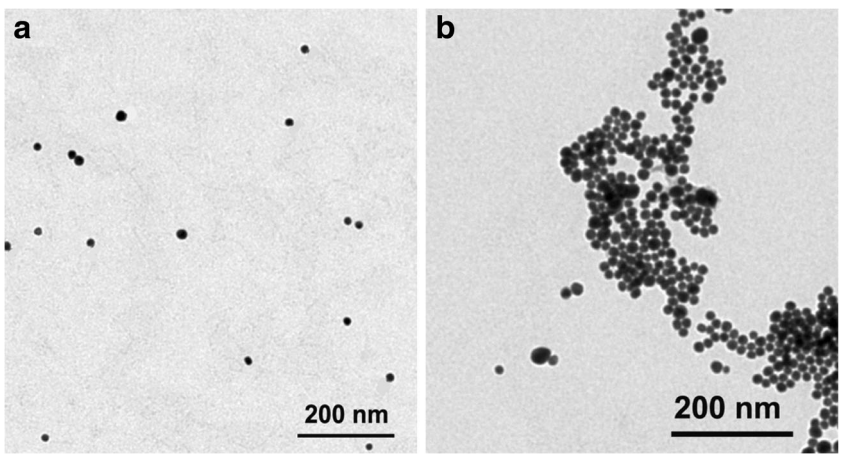

Fig. 1 Typical TEM images of AuNP solution containing (**a**) 0, and (**b**) 100 nM adenosine. NaCl concentration: 25 mM, Exo III concentration: 0.5 U/μL, HP1 concentration: 40 nM, HP2 concentration: 100 nM, and pH = 7.0

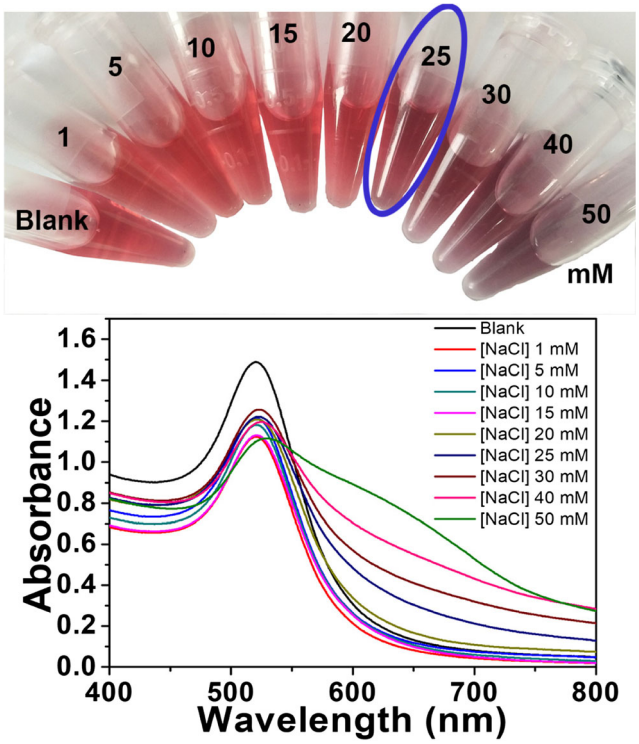

Fig. 2 The effect of different concentrations of NaCl on (**a**) The color, (**b**) UV-vis spectra of HP1-AuNP solution. Exo III concentration: 0.5 U/μL, HP1 concentration: 40 nM, HP2 concentration: 100 nM, and pH = 7.0

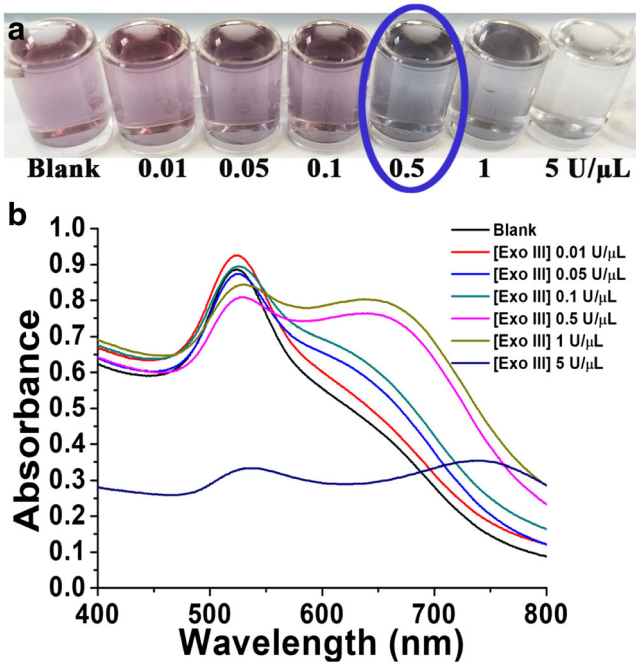

Fig. 3 The effect of different concentrations of Exo III on (**a**) The color, (**b**) UV-vis spectra of HP1-adenosine-HP2-AuNP solution. NaCl concentration: 25 mM, HP1 concentration: 40 nM, HP2 concentration: 100 nM, and pH = 7.0

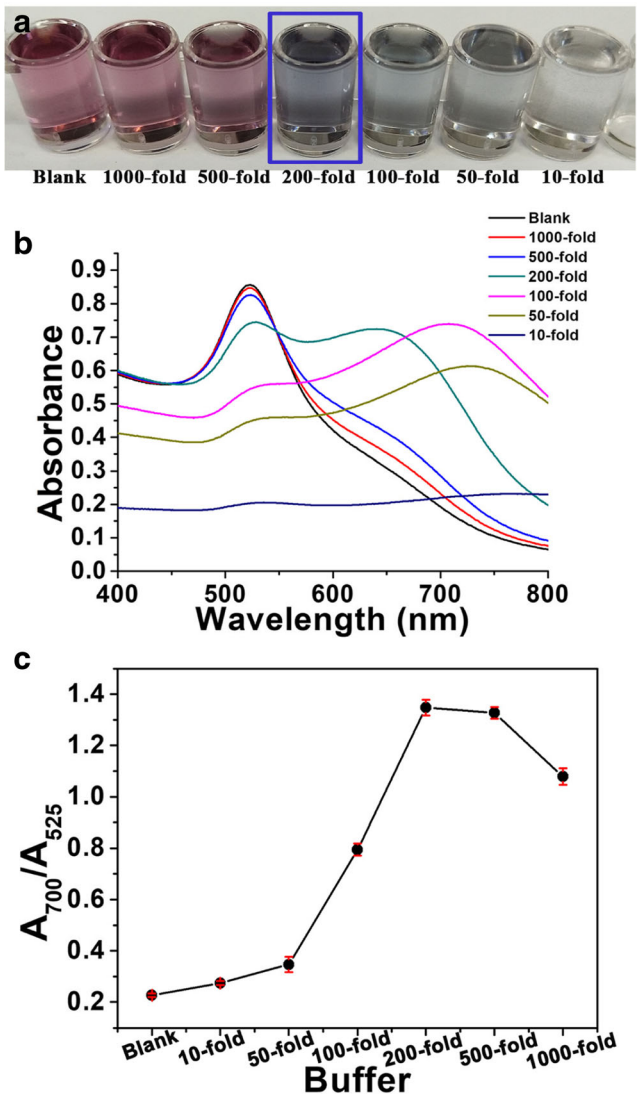

Fig. 4 The effect of different dilution multiples on (**a**) solution color, (**b**) UV-vis spectra, and (**c**) the A_{700}/A_{525} of HP1-adenosine-HP2-AuNP solution. The error bars represent standard deviation obtained from three independent measurements. NaCl concentration: 25 mM, Exo III concentration: 0.5 U/μL, HP1 concentration: 40 nM, HP2 concentration: 100 nM, and pH = 7.0

temperature to form the hairpin structures. 70 μL of HP1 (40 nM) was mixed with adenosine at various concentrations (final concentration: 0–5 μM) for incubation of 1 h at 37 °C. Afterwards, 70 μL of HP2 (100 nM) was injected to the solution and mixed thoroughly, followed by the addition of 70 μL of Exo III (0.5 U/μL) (pH 6.5) containing 200 mM KCl, 5 mM KPO_4, and 0.05 mM EDTA for another 2 h incubation at 37 °C. Then, 400 μL of AuNPs (10 nM) was added to the above solution. After incubation of 3 h at 37 °C, 18 μL of 1 M NaCl was added and mixed. The mixture was rest at room temperature for 5 min to finish the coloration process. Finally, the solutions were used for absorbance measurement at wavelengths of 525 and 700 nm.

Results and discussion

Optimization of experimental conditions

Herein, the effect of NaCl concentration on the sensing performance was first investigated. As shown in Fig. 2, the absorbance of AuNP-HP1 solution at 525 nm gradually decreased with the increasing NaCl concentration from 0 to 50 mM. It can be found that when NaCl concentration was 25 mM, color began to change from red to blue-purple, which indicates 25 mM NaCl can induce AuNP aggregation in the presence of 40 nM HP1. Thus, 25 mM NaCl was used for further studies. Exo III concentration is an important factor due to its effect on the performance of the signal amplification. From Fig. 3, it is obvious that the absorbance of AuNPs at 520 nm was decreased with increasing Exo III concentration from 0 to 5 U/μL. Beyond 0.5 U/μL, the color of the solution became colorless, this is because that excessive Exo III was adsorbed on the surface of AuNPs, resulting in further AuNP aggregation. Hence, 0.5 U/μL Exo III was employed. The effect of the multiplier of the dilution of the buffer (10 mM Bis Tris Propane-HCl. 10 mM $MgCl_2$, 1 mM DTT, pH 7.0) on its absorbance are shown in Fig. 4. The result shows that maximum signal at A_{700}/A_{525} was observed when the buffer was diluted 200 times. Beyond 200-fold dilution, the A_{700}/A_{525} value began to decrease on account of lower ionic strength. Thus, 200-fold diluted buffer was selected for all subsequent assays. We also investigated the absorbance change using the above buffer between pH 6 to pH 7.5 (Fig. 5). We find that when solution pH was 7.0, the A_{700}/A_{525} value reached the maximum. This indicates that the solution of pH = 7 was the most conducive to the binding of the HP1 to target adenosine. Finally, we investigated the effect of GRS concentration on the absorbance. As displayed in **Fig. S2**, the A_{700}/A_{525} increased with the increase of GRS concentration from 40 to 100 nM, followed by the decrease beyond GRS concentration of 100 nM. This is because that a surplus of GRS generated more negative charges, which cause greater repulsion between negatively charged AuNPs and GRS. Thereby, the 100 nM GRS was selected for the subsequent research.

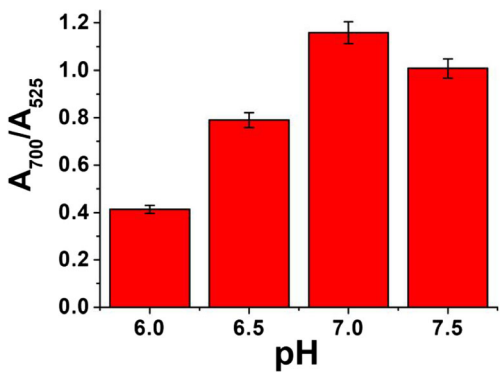

Fig. 5 The effect of solution pH on the absorbance change (A_{700}/A_{525}). NaCl concentration: 25 mM, Exo III concentration: 0.5 U/μL, HP1 concentration: 40 nM, and HP2 concentration: 100 nM. The error bars represent standard deviation obtained from three independent measurements

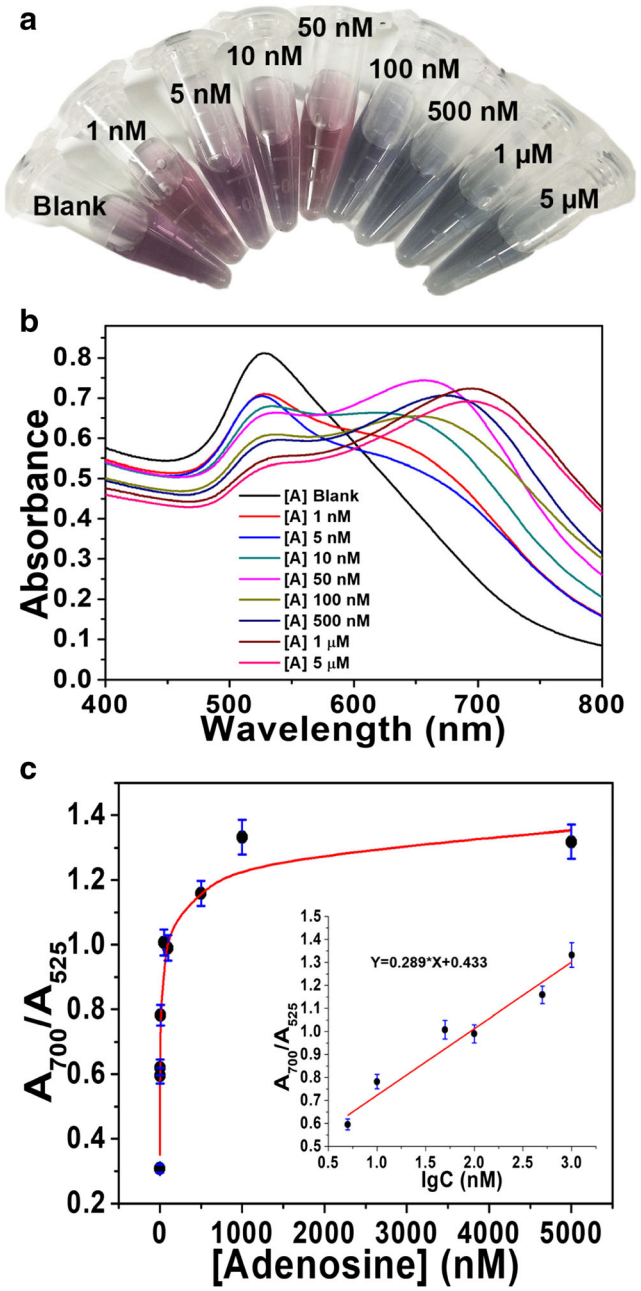

Fig. 6 **a** Photographs of the solution with different concentrations of adenosine. **b** UV-vis spectra of the solution upon the addition of various concentrations of adenosine from 0 to 5 μM. **c** Inset: calibration graph between A_{700}/A_{525} and log adenosine concentration (5 nM-1 μM). The error bars represent standard deviation obtained from three independent measurements

Table 1 Comparison of our method with other methods for adenosine detection

Material	Method	Detection limit (nM)	Linear range	Ref.
AuNPs, aptamer, and Exo III	Colorimetry	0.13	5 nM-1 μM	This work
Carbon dots and aptamer	Fluorescence	0.63	2–50 nM	[33]
CdTe quantum dots	Fluorescence	0.217	0.333–167 nM	[34]
Aptamer, Exo I and a 2-aminopurine-modified DNA	Fluorescence	300	10–600 μM	[35]
DNA/Ag nanoclusters	Fluorescence	103.4	0.5–7.0 μ M	[7]
Cu/Ag nanoclusters	Fluorescence	19	0–1 μ M	[36]
Exo III and aptamer	Colorimetry	17	50 nM-6 μM	[37]
Endonuclease, aptamer, and magnetic beads	Electrochemistry	0.032	0.05–20 nM	[38]

Analytical performance

To assess the sensitivity of the colorimetric sensor for determination of adenosine, under the optimized experimental conditions, as shown in Fig. 6a, b, we can observe that the AuNP solution undergoes a red-to-dark blue-to-colorless color change, and the absorbance values (A_{700}/A_{525}) gradually increase with the increase of adenosine concentration from 0 to 5 μM. However, at higher concentrations (1 μM), the detection signals gradually level off. The absorbance intensity (A_{700}/A_{525}) shows a good linear relationship with the logarithm of adenosine concentration in the range of 5 nM-1 μM (inset of Fig. 6c). The limit of detection (LOD) was estimated as 0.13 nM, calculated by three times signal to noise. Compared with other reported methods for adenosine detection, as shown in Table 1, the sensitivity of the assay was comparable or more sensitive.

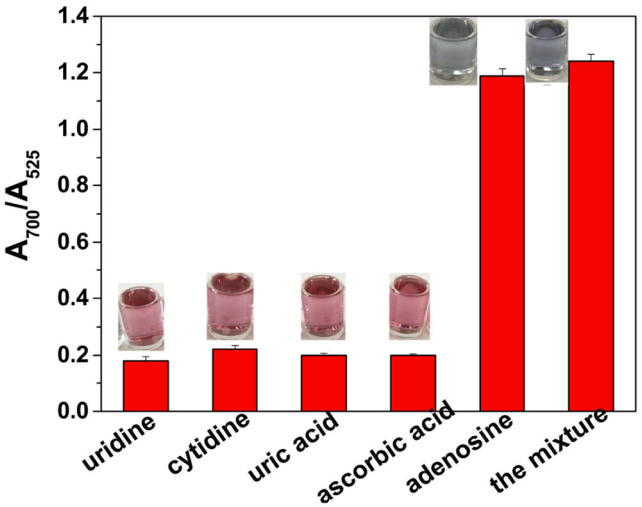

Fig. 7 Change in absorbance of the AuNP solution in the presence of adenosine and other interfering substance (uridine, cytidine, uric acid, and ascorbic acid). Inset: photograph of AuNP solutions in the presence of adenosine and its analogues. The concentrations of analogues (500 μM) were 100-fold higher than that of adenosine (5 μM). The error bars represent standard deviation obtained from three independent measurements

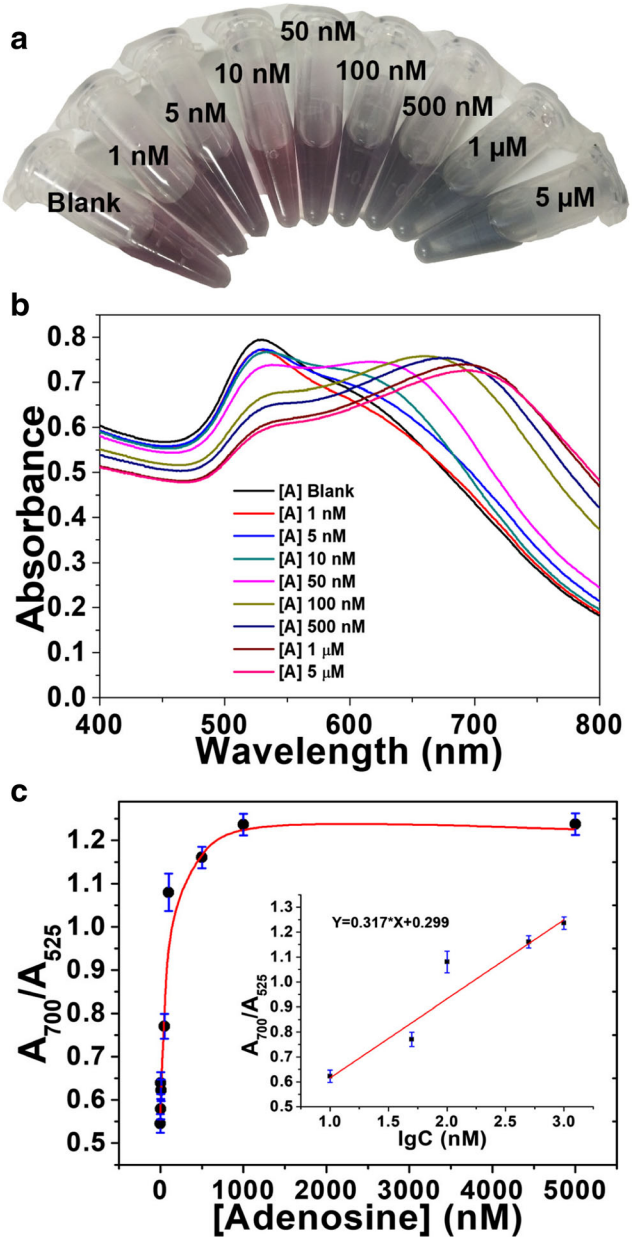

Fig. 8 **a** Photographs of AuNP solution before and after addition of different concentrations of adenosine. **b** Changes of absorption spectra after the addition of adenosine with various concentrations. **c** The different absorbance intensity (A_{700}/A_{525}) corresponding to different concentrations of adenosine. Inset: linear calibration plot for adenosine detection in urine samples. Error bars indicate standard deviation of the mean of three experiments

Table 2 The values of adenosine spiked in human urine samples and determination using the sensor ($n = 3$)

Urine samples	Adenosine spiked (nM)	Detected by this sensor (nM)	Recovery rate (%)
1	50	46.88	93.76
2	500	495.65	99.13
3	1000	947	94.70

Selectivity

To test the selectivity of this adenosine detection method, the absorbance intensity values (A_{700}/A_{525}) of two analogues of adenosine including uridine (U) and cytidine (C), uric acid, and ascorbic acid were measured, respectively. As shown in Fig. 7, the addition of 500 μM these interfering substance, which was 100-fold higher than that of adenosine, to the solutions did not produce remarkable absorbance, which was negligible compared with the absorbance intensity of adenosine. In addition, the coexistence of adenosine and these interfering substance show almost identical absorbance generated by adenosine, demonstrating that the specificity of this sensor was reasonably satisfactory for target adenosine. The good selectivity was ascribed to a high affinity of the HP1 for adenosine.

Analytical application

To demonstrate the feasibility of this sensing system in practical applications, human urine samples were collected from our laboratory staff. The need for working in the UV makes the probe prone to interferences by biomatter (in blood/serum, cells, marine water, wastewaters etc.) which always display strong background UV absorption and fluorescence. In addition, the UV light used for excitation may be screened off by UV absorbing biomolecules. In view of the above considerations, prior to measurement, the urine samples were centrifuged at 12000 rpm for 10 min and diluted 100 times to reduce the impact of interfering substance on adenosine detection.Then the urine samples were spiked with adenosine at different concentration levels (final concentrations: 0, 1, 5, 10, 50, 100, 500, 1000, and 5000 nM). The measurement procedure of adenosine detection in urine samples is the same as that in buffer. A linear regression equation for adenosine, $A_{700}/A_{525} = 0.317\lg C + 0.299$ ($R = 0.97$), was obtained when the concentration of adenosine was in the range of 1 nM-1 μM (Fig. 8). In addition, according to the recovery rates obtained from urine samples, as shown in Table 2, it shows that the detection results were consistent with the spiked adenosine concentrations, satisfying the practical adenosine detection in real samples.

Conclusion

In summary, a novel colorimetric aptasensor for adenosine detection, which is based on Exo III-assisted DNA cycling amplification and G-quadruplex-induced AuNP aggregation in salt solution. The developed sensor can sensitively and selectively detect adenosine due to the signal amplified effect and the recognition function of aptamers. The red-to-blue color change can be monitored or visualized with the satisfying detection limit of 0.13 nM, and the assay can discriminate adenosine from other interfering substance with high selectivity. Although the aptasensor possesses excellent sensitivity and selectivity, its application in real samples may be hampered by the relatively long reaction time (2 h), which requires further study.

Acknowledgements This study was supported by Scientific Research Project of Beijing Educational Committee (Grant No. KM201710028009), Youth Innovative Research Team of Capital Normal University, and Capacity Building for Sci-Tech Innovation-Fundamental Scientific Research Funds (025185305000/195).

Compliance with ethical standards The author(s) declare that they have no competing interests.

References

1. Latini S, Pedata F (2001) Adenosine in the central nervous system: release mechanisms and extracellular concentrations. J Neurochem 79:463–484
2. Cunha RA (2001) Adenosine as a neuromodulator and as a homeostatic regulator in the nervous system: different roles, different sources and different receptors. Neurochem Int 38:107–125
3. Nguyen MD, Venton BJ (2015) Fast-scan cyclic voltammetry for the characterization of rapid adenosine release. Comput Struct Biotechnol J 13:47–54
4. Borea PA, Gessi S, Merighi S, Varani K (2016) Adenosine as a multi-signalling guardian angel in human diseases: when, where and how does it exert its protective effects? Trends Pharmacol Sci 37:419–434
5. Yin D, Liu YY, Wang TX, Hu ZZ, Qu WM, Chen JF, Cheng NN, Huang ZL (2016) Paeoniflorin exerts analgesic and hypnotic effects via adenosine a(1) receptors in a mouse neuropathic pain model. Psychopharmacology 233:281–293
6. Majetschak M (2016) Multiple ways of targeting the adenosine/adenosine receptor axis in lung inflammation and injury. Crit Care Med 44(2016):853–854
7. Zhu Y, Hu XC, Shi S, Gao RR, Huang HL, Zhu YY, Lv XY, Yao TM (2016) Ultrasensitive and universal fluorescent aptasensor for the detection of biomolecules (ATP, adenosine and thrombin) based

on DNA/ag nanoclusters fluorescence light-up system. Biosens Bioelectron 79:205–212
8. Hashemian Z, Khayamian T, Saraji M, Shirani MP (2016) Aptasensor based on fluorescence resonance energy transfer for the analysis of adenosine in urine samples of lung cancer patients. Biosens Bioelectron 79:334–340
9. Song YY, Xu GH, Wei FD, Cen Y, Sohail M, Shi ML, Xu XM, Ma YS, Ma YJ, Hu Q (2018) Aptamer-based fluorescent platform for ultrasensitive adenosine detection utilizing Fe_3O_4 magnetic nanoparticles and silver nanoparticles. Microchim Acta 185:139
10. Li LL, Ge PH, Selvin PR, Lu Y (2012) Direct detection of adenosine in undiluted serum using a luminescent aptamer sensor attached to a terbium complex. Anal Chem 84:7852–7856
11. Shi HW, Wu MS, Du Y, Xu JJ, Chen HY (2014) Electrochemiluminescence aptasensor based on bipolar electrode for detection of adenosine in cancer cells. Biosens Bioelectron 55: 459–463
12. Fang HF, Pajski ML, Ross AE, Venton BJ (2013) Quantitation of dopamine, serotonin and adenosine content in a tissue punch from a brain slice using capillary electrophoresis with fast-scan cyclic voltammetry detection. Anal Methods-Uk 5:2704–2711
13. Jeon JS, Kim HT, Kim MG, Oh MS, Hong SR, Yoon MH, Cho SM, Shin HC, Shim JH, Ramadan A, Abd El-Aty AM (2016) Simultaneous determination of watersoluble whitening ingredients and adenosine in different cosmetic formulations by high-performance liquid chromatography coupled with photodiode array detection. Int J Cosmet Sci 38:286–293
14. Fu LJ, Amato NJ, Wang PC, McGowan SJ, Niedernhofer LJ, Wang YS (2015) Simultaneous quantification of methylated cytidine and adenosine in cellular and tissue RNA by nano-flow liquid chromatography-tandem mass spectrometry coupled with the stable isotope-dilution method. Anal Chem 87:7653–7659
15. Zhang C, Man BY, Jiang SZ, Yang C, Liu M, Chen CS, Xu SC, Qiu HW, Li Z (2015) SERS detection of low-concentration adenosine by silver nanoparticles on silicon nanoporous pyramid arrays structure. Appl Surf Sci 347:668–672
16. Yao G, Liang R, Huang C, Zhang L, Qiu J (2015) Enzyme-free surface Plasmon resonance aptasensor for amplified detection of adenosine via target-triggering strand displacement cycle and au nanoparticles. Anal Chim Acta 871:28–34
17. Ye SJ, Li HX, Cao W (2011) Electrogenerated chemiluminescence detection of adenosine based on triplex DNA biosensor. Biosens Bioelectron 26:2215–2220
18. Chen JW, Liu XP, Feng KJ, Liang Y, Jiang JH, Shen GL, Yu RQ (2008) Detection of adenosine using surface-enhanced Raman scattering based on structure-switching signaling aptamer. Biosens Bioelectron 24:66–71
19. Yan FF, Wang F, Chen ZL (2011) Aptamer-based electrochemical biosensor for label-free voltammetric detection of thrombin and adenosine. Sensors Actuators B Chem 160:1380–1385
20. Wang YT, Feng JJ, Tan ZA, Wang HY (2014) Electrochemical impedance spectroscopy aptasensor for ultrasensitive detection of adenosine with dual backfillers. Biosens Bioelectron 60:218–223
21. Li F, Zhang J, Cao X, Wang LH, Li D, Song SP, Ye BC, Fan CH (2009) Adenosine detection by using gold nanoparticles and designed aptamer sequences. Analyst 134:1355–1360
22. Chen SJ, Huang YF, Huang CC, Lee KH, Lin ZH, Chang HT (2008) Colorimetric determination of urinary adenosine using aptamer-modified gold nanoparticles. Biosens Bioelectron 23: 1749–1753
23. Liu JW, Lu Y (2004) Adenosine-dependent assembly of aptazyme-functionalized gold nanoparticles and its application as a colorimetric biosensor. Anal Chem 76:1627–1632
24. Ding YN, Yang BC, Liu H, Liu ZX, Zhang X, Zheng XW, Liu QY (2018) FePt-au ternary metallic nanoparticles with the enhanced peroxidase-like activity for ultrafast colorimetric detection of H_2O_2. Sensors Actuators B Chem 259:775–783
25. Liu DB, Wang Z, Jiang XY (2011) Gold nanoparticles for the colorimetric and fluorescent detection of ions and small organic molecules. Nanoscale 3:1421–1433
26. Liu JW, Lu Y (2003) A colorimetric lead biosensor using DNAzyme-directed assembly of gold nanoparticles. J Am Chem Soc 125:6642–6643
27. Liu DB, Qu WS, Chen WW, Zhang W, Wang Z, Jiang XY (2010) Highly sensitive, colorimetric detection of mercury(II) in aqueous media by quaternary ammonium group-capped gold nanoparticles at room temperature. Anal Chem 82:9606–9610
28. Nam JM, Wise AR, Groves JT (2005) Colorimetric bio-barcode amplification assay for cytokines. Anal Chem 77:6985–6988
29. Liu QY, Yang YT, Li H, Zhu RR, Shao Q, Yang SG, Xu JJ (2015) NiO nanoparticles modified with 5,10,15,20-tetrakis(4-carboxyl pheyl)-porphyrin: promising peroxidase mimetics for H_2O_2 and glucose detection. Biosens Bioelectron 64:147–153
30. Klajn R, Stoddart JF, Grzybowski BA (2010) Nanoparticles functionalised with reversible molecular and supramolecular switches. Chem Soc Rev 39:2203–2237
31. Du LL, Zhang Y, Du Y, Yang DZ, Gao FL, Tang DQ (2015) A novel label-free aptasensor based on target-induced structure switching of aptamer-functionalized mesoporous silica nanoparticles. RSC Adv 5:100960–100967
32. Gao FL, Du Y, Yao JW, Zhang YZ, Gao J (2015) A novel electrochemical biosensor for DNA detection based on exonuclease III-assisted target recycling and rolling circle amplification. RSC Adv 5:9123–9129
33. Wang X, Xu GH, Wei FD, Ma YS, Ma YJ, Song YY, Cen Y, Hu Q (2017) Highly sensitive and selective aptasensor for detection of adenosine based on fluorescence resonance energy transfer from carbon dots to nano-graphite. J Colloid Interf Sci 508:455–461
34. Song YY, Tang T, XWang X, Xu GH, Wei FD, Wu YZ, Song Q, Ma YJ, Ma YS, Cen Y, Hu Q (2017) Highly selective and sensitive detection of adenosine utilizing signal amplification based on silver ions-assisted cation exchange reaction with CdTe quantum dots. Sensors Actuators B Chem 247:305–311
35. Liu HY, Bai YF, Qin J, Wang HY, Wang YZ, Chen ZZ, Feng F (2018) Exonuclease I assisted fluorometric aptasensor for adenosine detection using 2-AP modified DNA. Sensors Actuators B Chem 256:413–419
36. Ahn JK, Kim HY, Baek S, Park HG (2017) A new s-adenosylhomocysteine hydrolase-linked method for adenosine detection based on DNA-templated fluorescent Cu/Ag nanoclusters. Biosens. Bioelectron 93:330–334
37. Xu L, Shen X, Li BZ, Zhu CH, Zhou XM (2017) G-quadruplex based Exo III-assisted signal amplification aptasensor for the colorimetric detection of adenosine. Anal Chim Acta 980:58–64
38. Shen J, Wang HY, Li CX, Zhao YY, Yu XJ, Luo XL (2017) Label-free electrochemical aptasensor for adenosine detection based on cascade signal amplification strategy. Biosens Bioelectron 90:356–362